Supporting Information For

The first study of the thermal and storage stability of arenediazonium triflates comparing to 4-nitrobenzenediazonium tosylate and tetrafluoroborate by calorimetric methods

Alexander A. Bondarev[1], Evgeny V. Naumov[1], AssiyaZh. Kassanova[2], Elena A. Krasnokutskaya[3], Ksenia S. Stankevich[3], Victor D. Filimonov[3]**

[1] Department of Biomedicine, Altai State University, Barnaul, Russia, alex_root@mail.ru

[2] S. Toraighyrov Pavlodar State University, Pavlodar, Kazakhstan

[3] The Kizhner Research Center,National ResearchTomsk Polytechnic University, Tomsk, Russian Federation

1s. Results of modeling and deconvolution of heat flow experimental kinetic curves acquired in isothermal conditions

Deconvolution was performed by computer simulation of combinations of two independent and two consecutive autocatalytic reactions with varying values of thermal effects and kinetic parameters and minimization of the standard deviation from the experimental curve using the Broyden–Fletcher–Goldfarb–Shanno algorithm (BFGS)[1a] implemented in our computer program,[1b] as well as Nelder–Mead [1c] method implemented in the R statistics software package for statistical analysis and processing.[2] The initial values for the first approximation were taken from the DSC-TGA data (endothermic reaction). Figures 1s.1-6 show the results of

deconvolution. The model of two independent autocatalytic processes was found to describe the experimental dependencies more accurately.

Table S1. The result of the deconvolution of the heat flow measured during the isothermal decomposition of 2-nitrobenzenediazonium triflate **1a** using the model of two independent autocatalytic processes.

T °C	k_1	k_2	C_{01}	C_{02}	dH_1	dH_2	Quality
75	0.5222	0.0480	0.00133	0.00304	48.5	-500.6	$7.3 \cdot 10^{-10}$
80	0.4046	0.0489	0.00111	0.00230	30.7	-441.0	$7.1 \cdot 10^{-9}$
85	0.9554	0.0611	0.00070	0.00272	32.5	-453.9	$1.3 \cdot 10^{-8}$

Table S2. The result of the deconvolution of the heat flow measured during the isothermal decomposition of 2-nitrobenzenediazonium triflate **1a** using the model of two consecutive autocatalytic processes.

T °C	k_1	k_2	C_{01}	C_{02}	dH_1	dH_2	Quality
75	0.4679	0.0642	0.00191	0.00204	39.2	-520.7	$1.1 \cdot 10^{-9}$
80	0.5791	0.0435	0.00122	0.00263	36.7	-493.9	$6.1 \cdot 10^{-9}$
85	1.0512	0.0631	0.00075	0.00259	31.8	-483.4	$1.3 \cdot 10^{-8}$

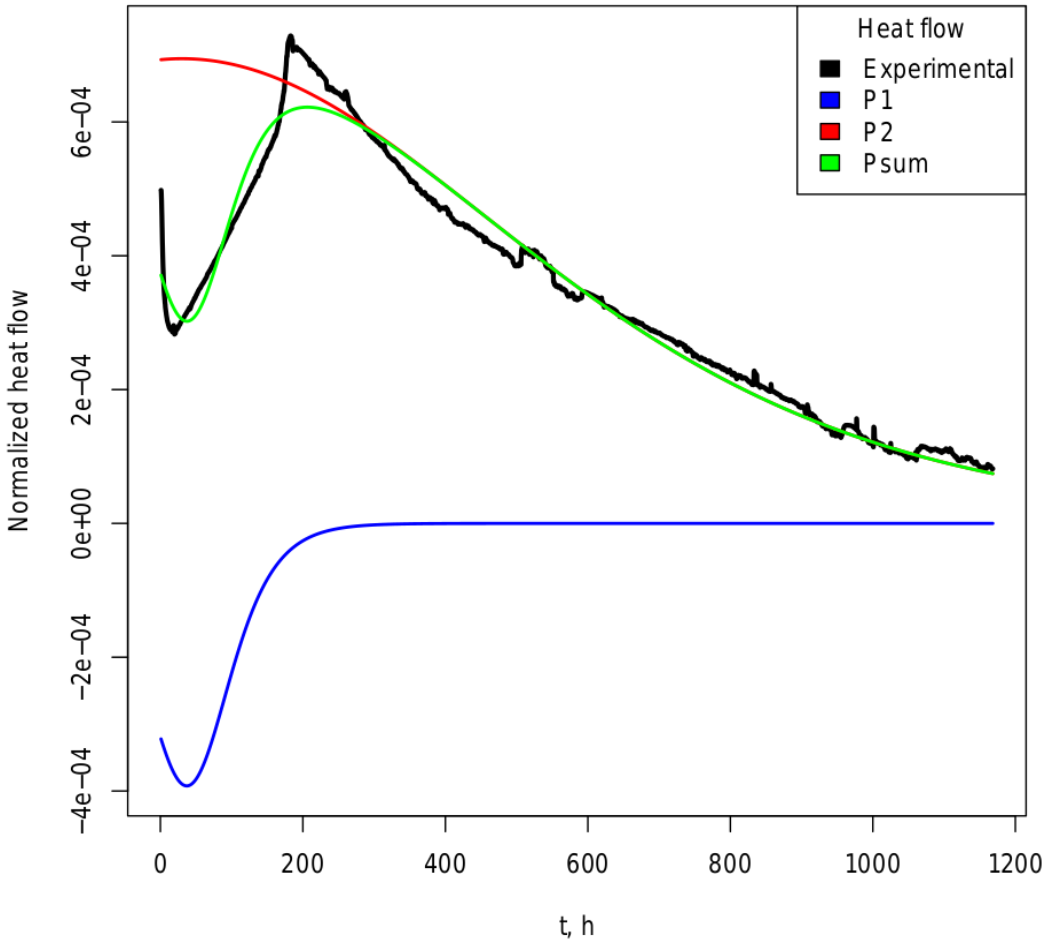

Figure S1. The heat flow experimental curve and its deconvolution results for the isothermal decomposition of 2-nitrobenzenediazonium triflate **1a** at 75 °C. The deconvolution was done using the model of two independent autocatalytic processes.

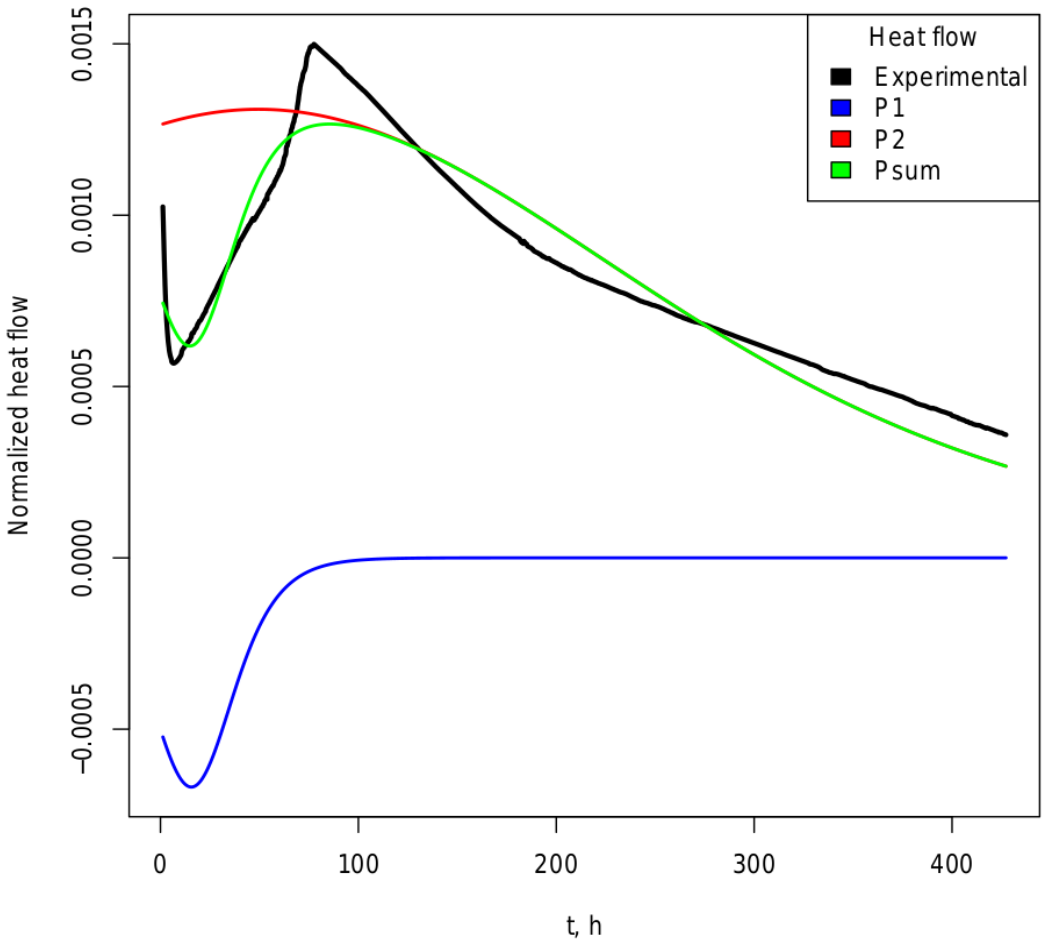

Figure S2. The heat flow experimental curve and its deconvolution results for the isothermal decomposition of 2-nitrobenzenediazonium triflate **1a** at 80 °C. The deconvolution was done using the model of two independent autocatalytic processes.

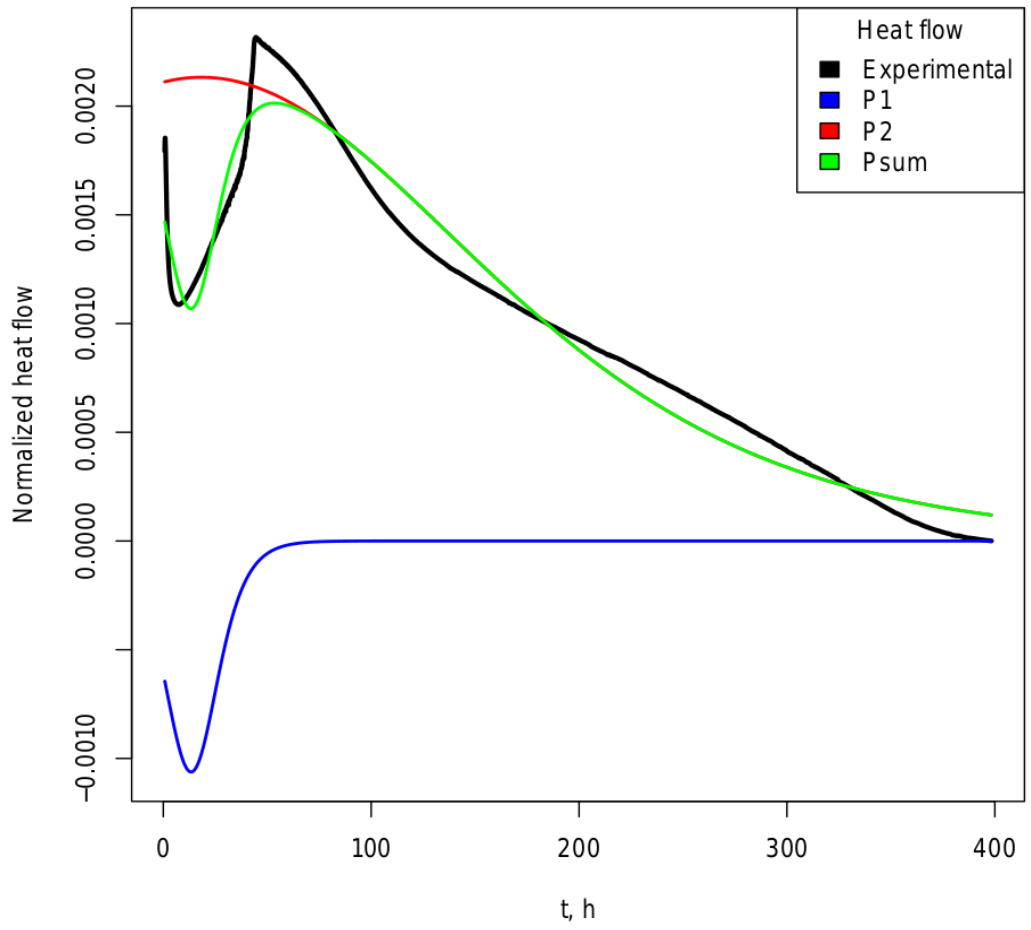

Figure S3. The heat flow experimental curve and its deconvolution results for the isothermal decomposition of 2-nitrobenzenediazonium triflate **1a** at 85 °C. The deconvolution was done using the model of two independent autocatalytic processes.

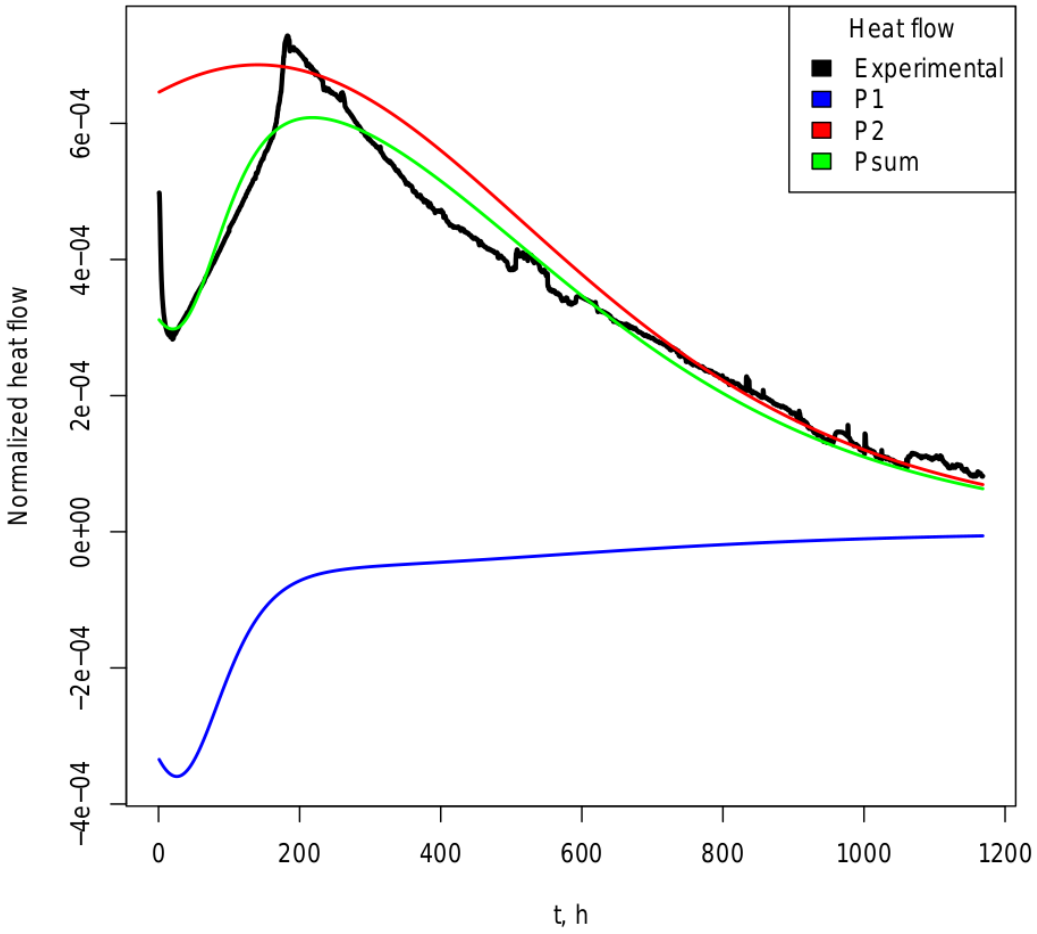

Figure S4. The heat flow experimental curve and its deconvolution results for the isothermal decomposition of 2-nitrobenzenediazonium triflate **1a** at 75 °C. The deconvolution was done using the model of two consecutive autocatalytic processes.

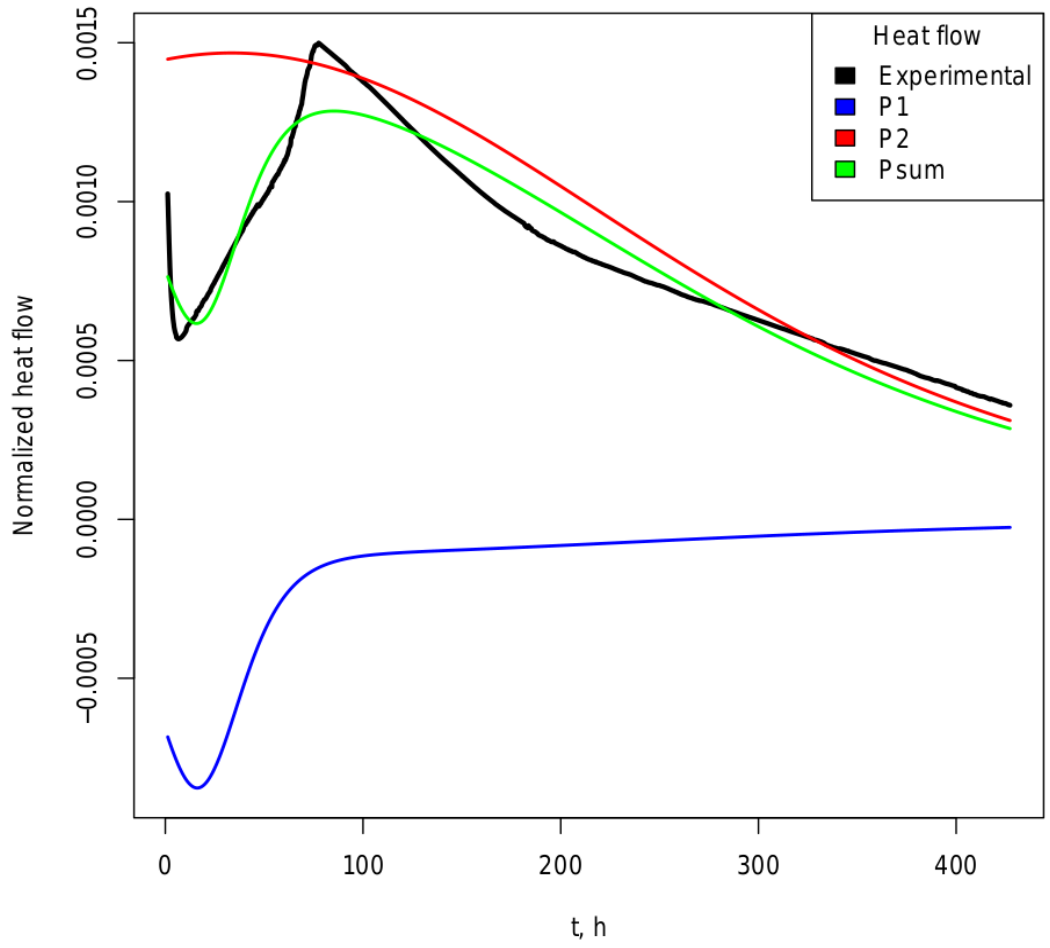

Figure S5. The heat flow experimental curve and its deconvolution results for the isothermal decomposition of 2-nitrobenzenediazonium triflate **1a** at 80 °C. The deconvolution was done using the model of two consecutive autocatalytic processes.

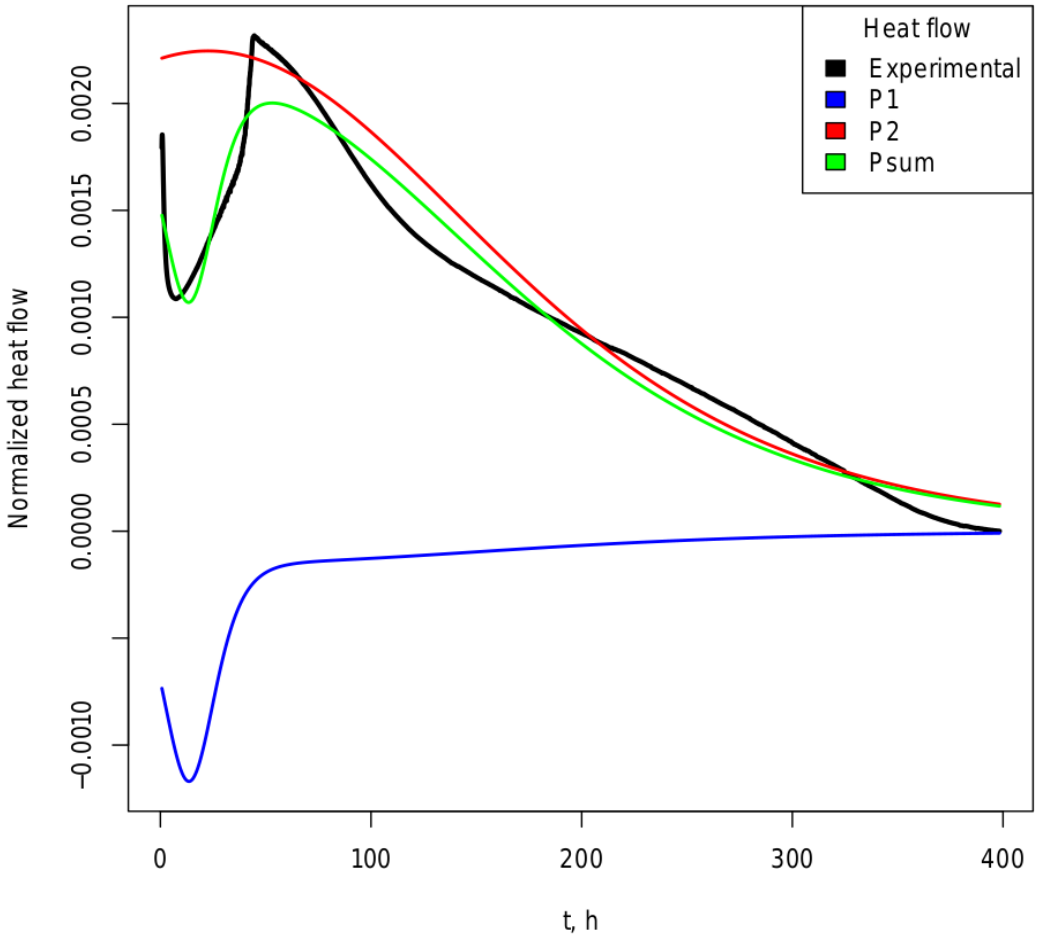

Figure S6. The heat flow experimental curve and its deconvolution results for the isothermal decomposition of 2-nitrobenzenediazonium triflate **1a** at 85 °C. The deconvolution was done using the model of two consecutive autocatalytic processes.

REFERENCES

Perry, R. H.; Green, D. W. Perry's Chemical Engineers' Handbook; The McGraw-Hill: 1999.

(1) (a) Fletcher, R. Practical methods of optimization (2nd ed.), New York: John Wiley & Sons: 1987, ISBN 978-0-471-91547-8, (b) Bondarev, A. Deconvolution-Kinetic. Zenodo November 7, **2018**. https://doi.org/10.5281/zenodo.1478946, (c) Nelder, J.

A.; Mead, R. A Simplex Method for Function Minimization. The Computer Journal **1965**, 7 (4), 308–313. https://doi.org/10.1093/comjnl/7.4.308.

(2) (a) Williams, T.; Kelley, C. Gnuplot 4.5: an interactive plotting program. URL http://gnuplot.info. 2011, (b) R Core Team. R: A language and environment for statistical computing. R Foundation for Statistical / Computing, Vienna, Austria. URL https://www.R-project.org/, 2017

Supporting 2s. GC-MS spectra of the decomposition products of diazonium salts studied

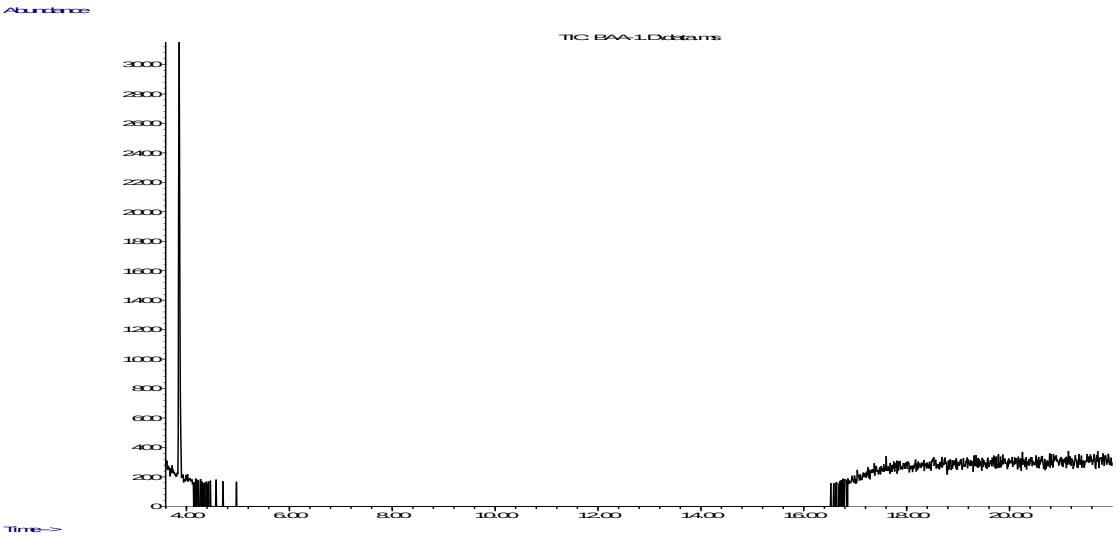

Figure S7. The decomposition products of DS **1a** according to GC-MS data.

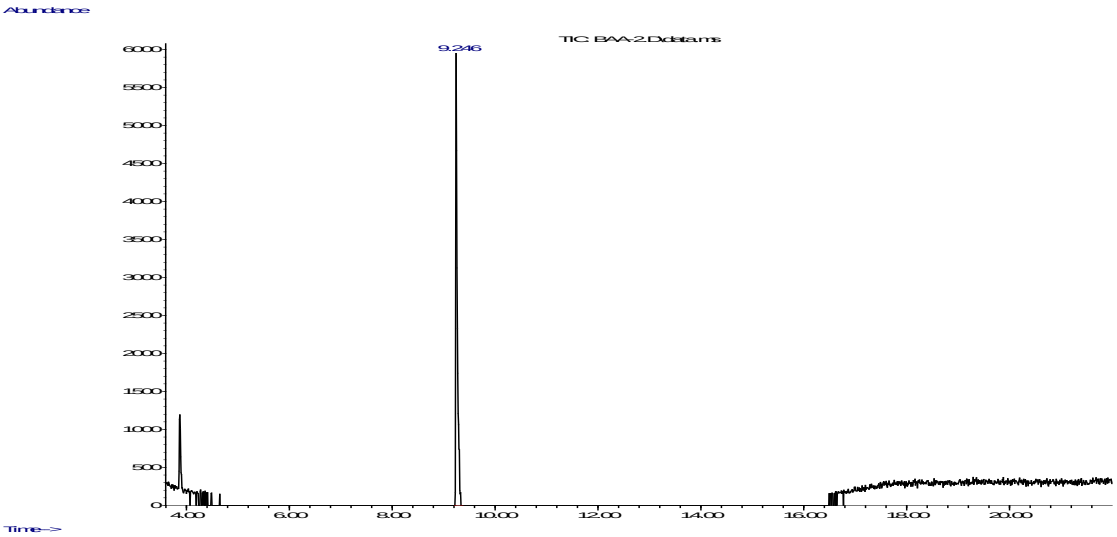

Figure S8. The decomposition products of DS **1b** according to GC-MS data. (Peak at 9.246 min corresponds to compound 3-NO_2-C_6H_4-OSO_2CF_3, Fig. 21)

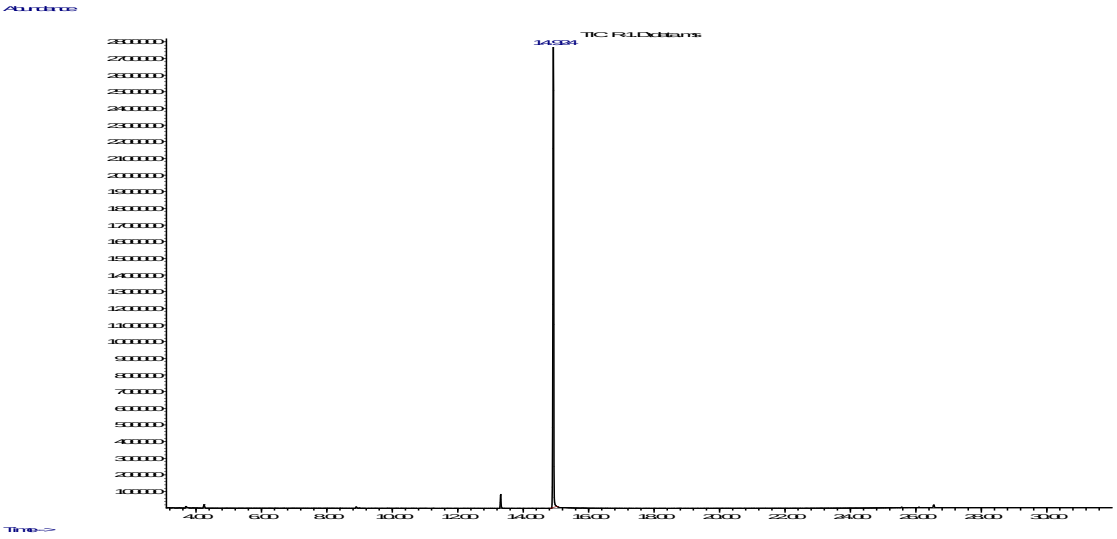

Figure S9. The decomposition products of DS **1c** according to GC-MS data. (Peak at 13.314 min corresponds to compound 4-NO_2-C_6H_4-OSO_2CF_3, peak at 14.912 min corresponds to compound 1-iodo-4-nitrobenzene, Fig. 22)

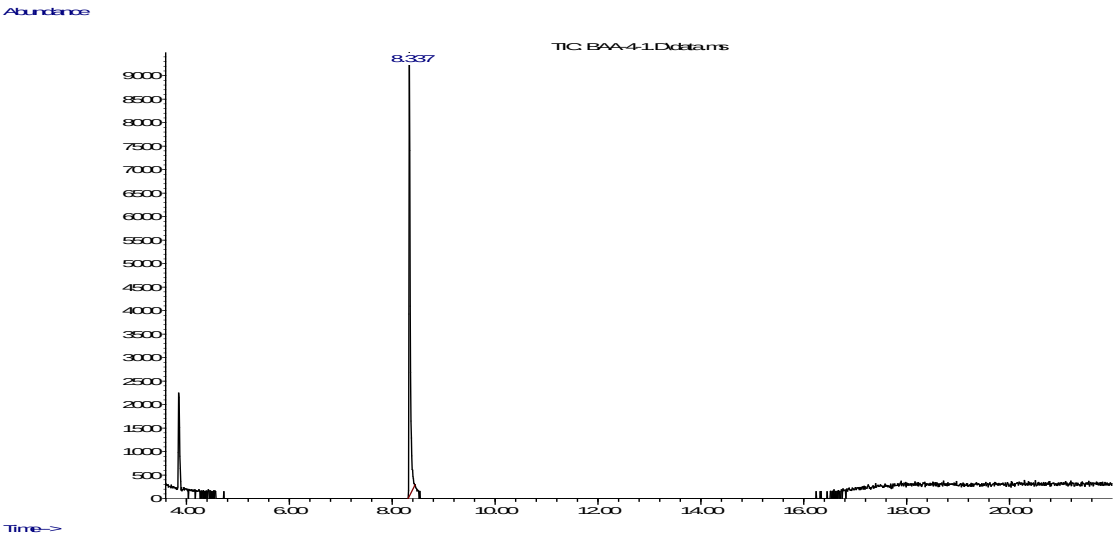

Figure S10. The decomposition products of DS **1d** according to GC-MS data. (Peak at 8.337 min corresponds to compound 4-CH_3O-C_6H_4-OSO_2CF_3, Fig. 23)

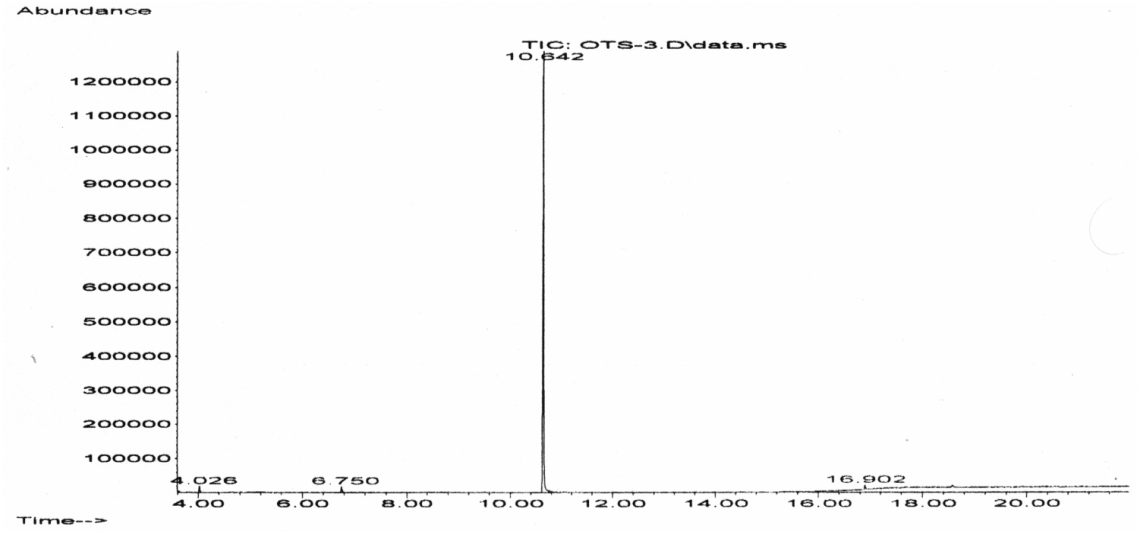

Figure S11. The decomposition products of DS **2** according to GC-MS data. (Peak at 6.750 min corresponds to 1-fluoro-4-nitrobenzene, peak at 10.642 min corresponds to 1-iodo-4-nitrobenzene, Fig. 24)

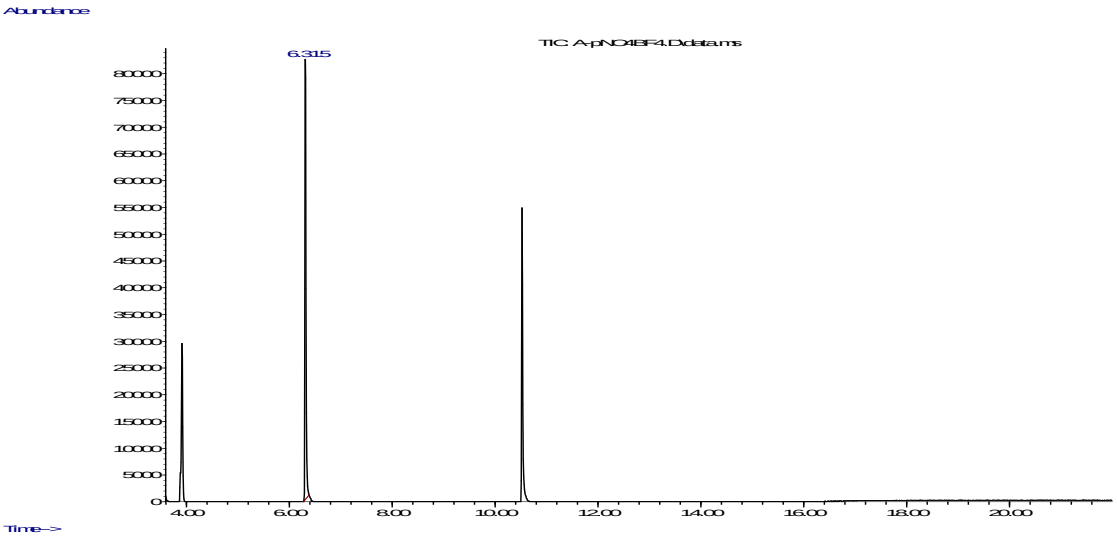

Figure S12. The decomposition products of DS **3** according to GC-MS data. (Peak at 6.307 min corresponds to 1-fluoro-4-nitrobenzene, peak at 10.515 min corresponds to 1-iodo-4-nitrobenzene, Fig. 25)

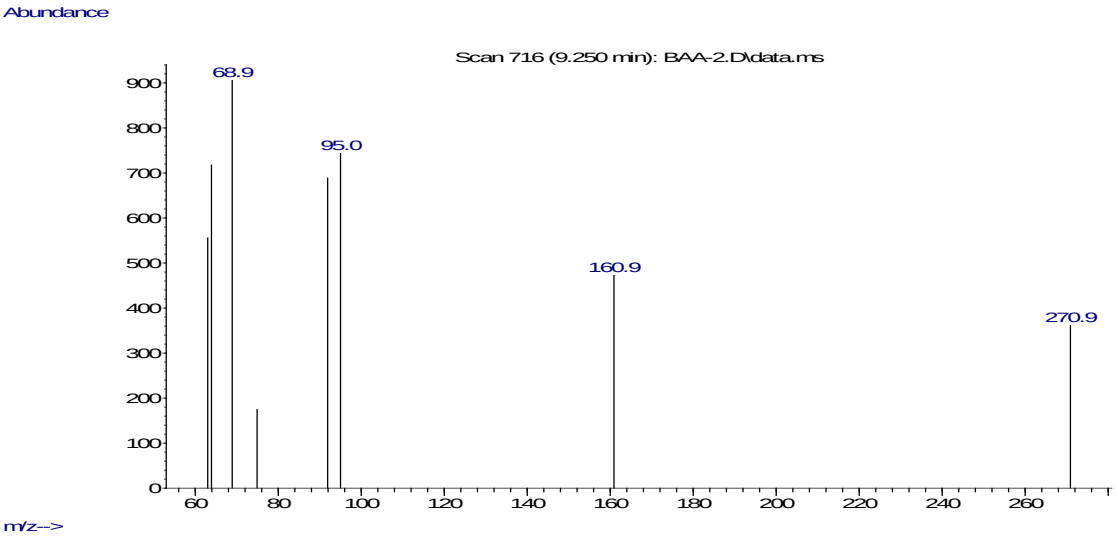

Figure S13. The major product of decomposition of DS **1b** according to GC-MS data. Fragmentation pattern corresponds to 3-NO_2-C_6H_4-OSO_2CF_3 M/Z: 271, 161, 95, 92, 69, 64.

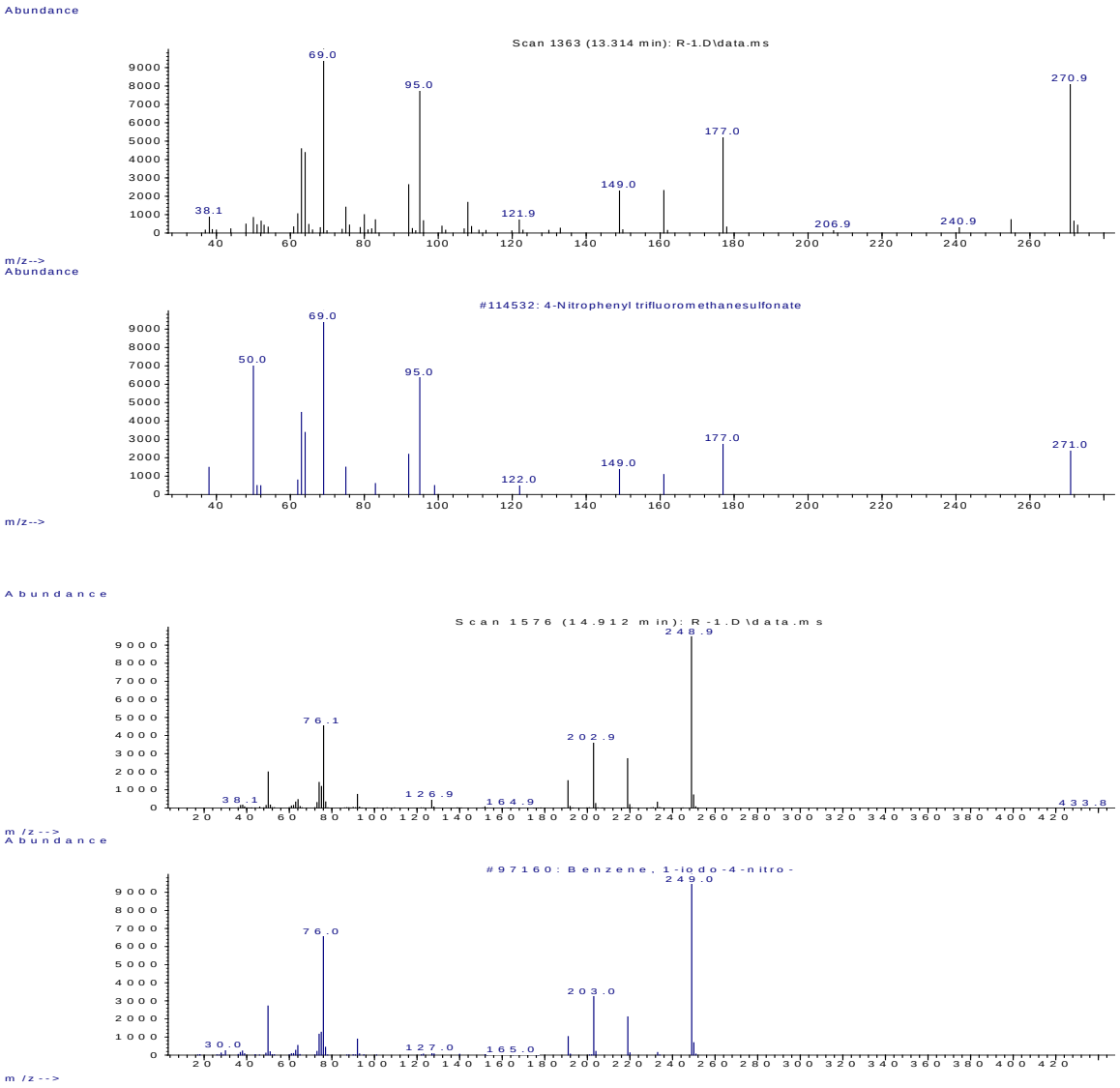

Figure S14. The major products of decomposition of DS **1c** according to GC-MS data. Fragmentation patterns correspond to 4-NO_2-C_6H_4-OSO_2CF_3 M/Z: 271, 177, 95, 69 and 1-iodo-4-nitrobenzene M/Z: 249, 203, 76.

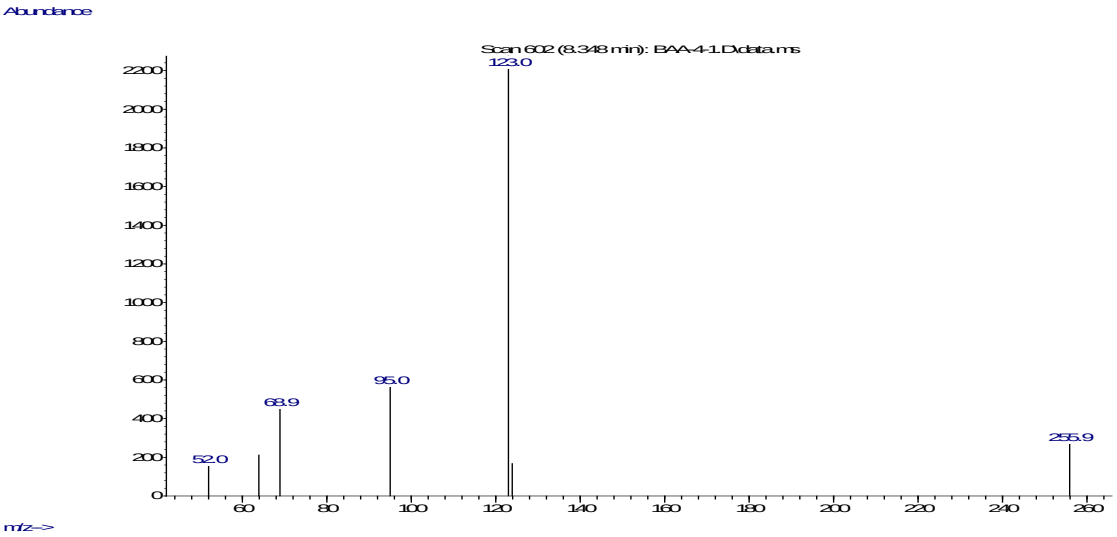

Figure S15. The major product of decomposition of DS 1d according to GC-MS data. Fragmentation pattern corresponds to 3-CH_3O-C_6H_4-OSO_2CF_3 M/Z: 256, 123, 69, 52.

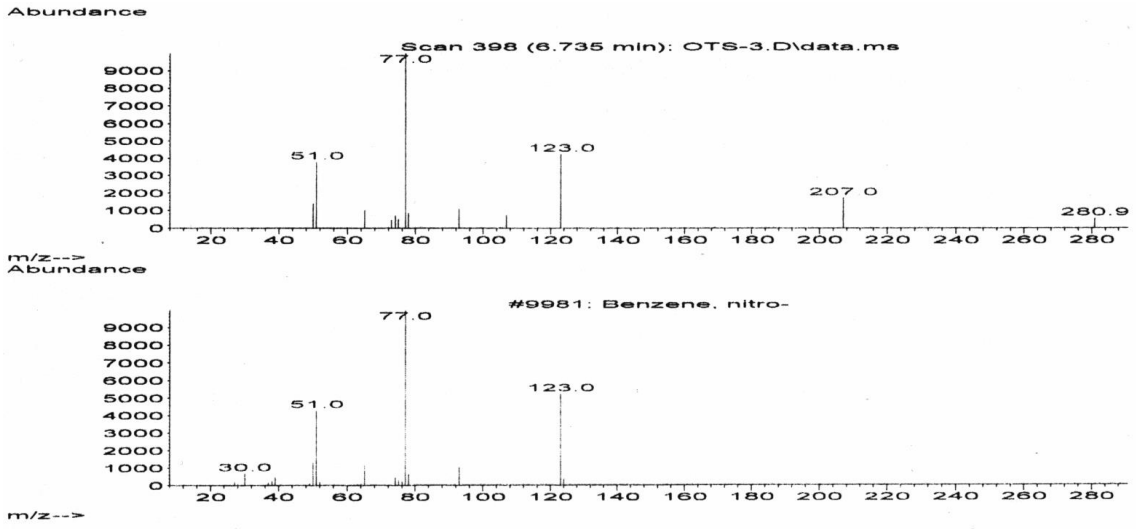

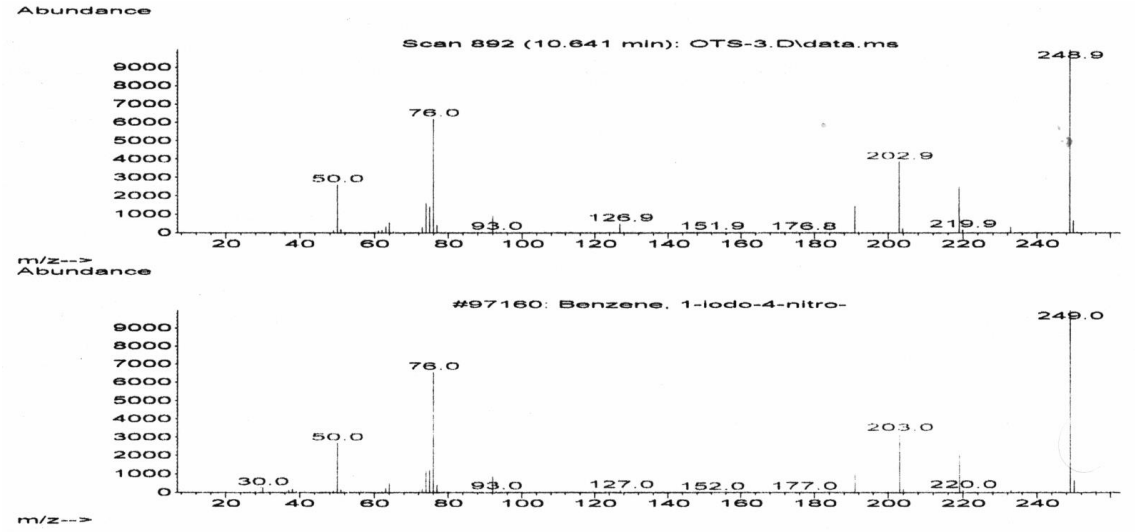

Figure S16. The major products of decomposition of DS 2 according to GC-MS data. Fragmentation patterns correspond to nitrobenzene M/Z: 123, 77, 51 and 1-iodo-4-nitrobenzene M/Z: 249, 203, 76, 50.

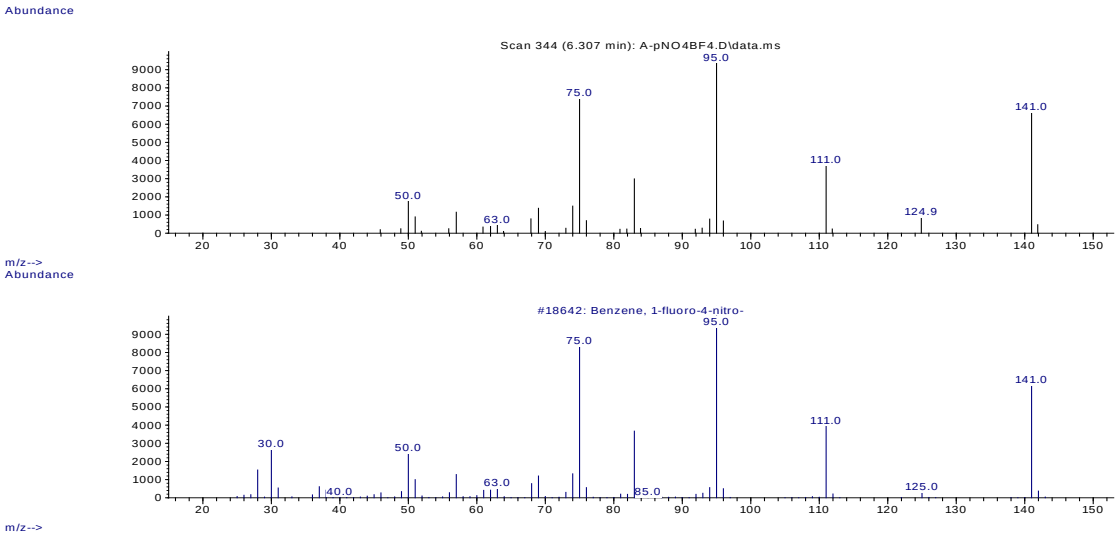

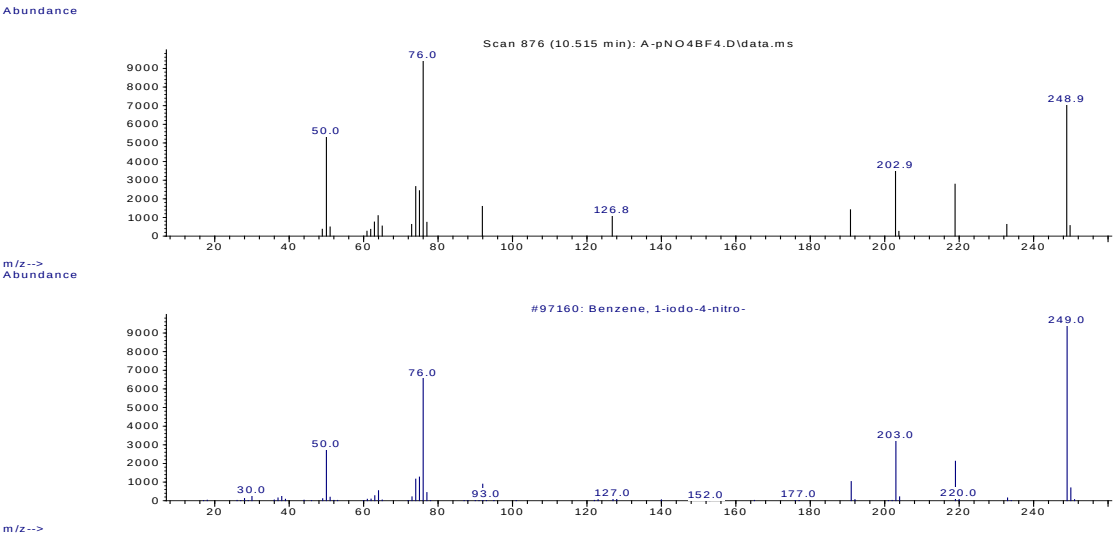

Figure S17. The major products of decomposition of DS **3** according to GC-MS data. Fragmentation patterns correspond to 1-fluoro-2-nitrobenzene M/Z: 141, 111, 95, 75, 50 and 1-iodo-4-nitrobenzene M/Z: 249, 203, 76.

Supporting 3s. LS-MS spectra of the decomposition products of diazonium salts studied

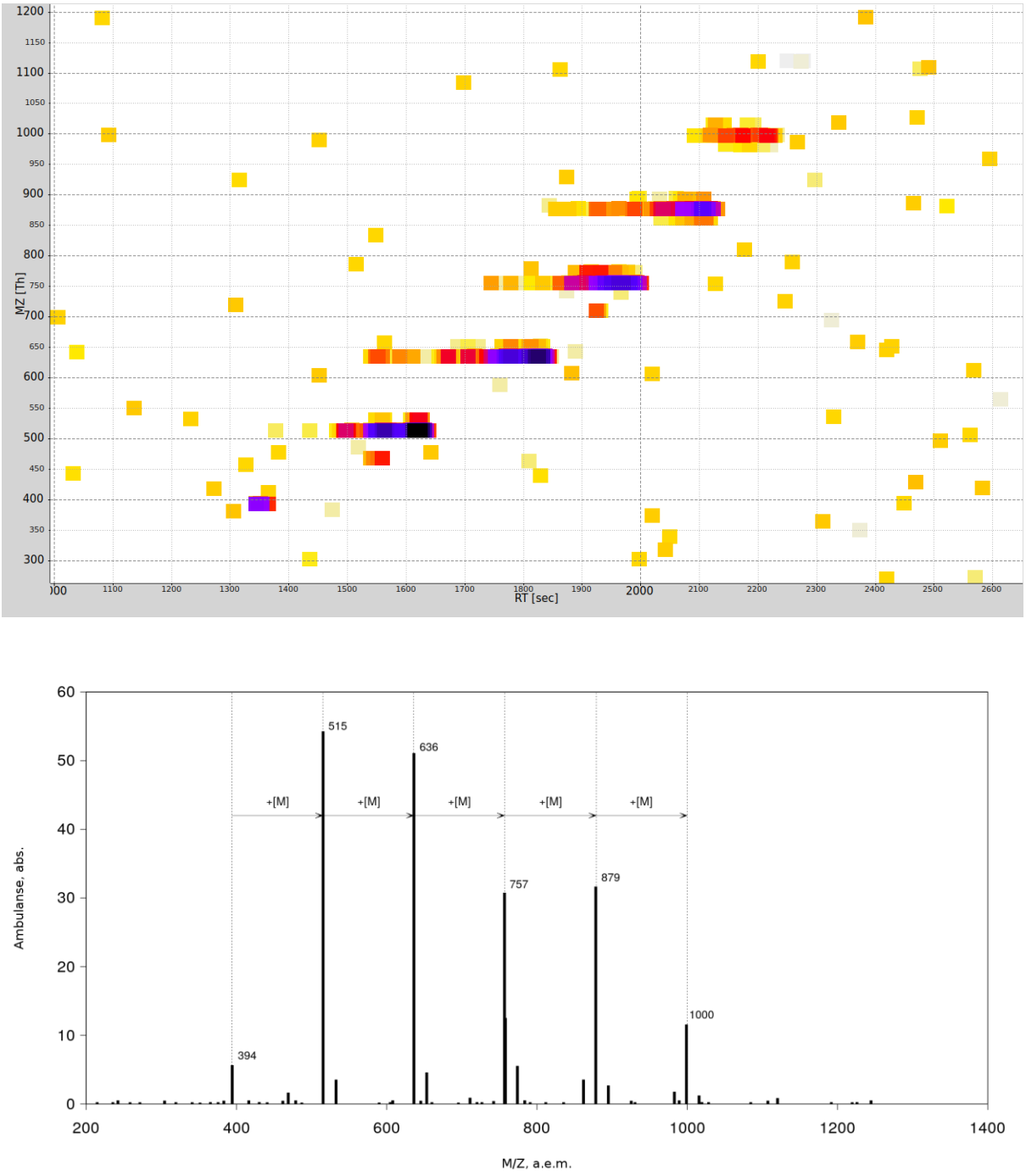

Figure S18. The chromatogram and the decomposition products of DS **1a** according to LC-MS data (APCI, Positive mode), M=$NO_2C_6H_3$.

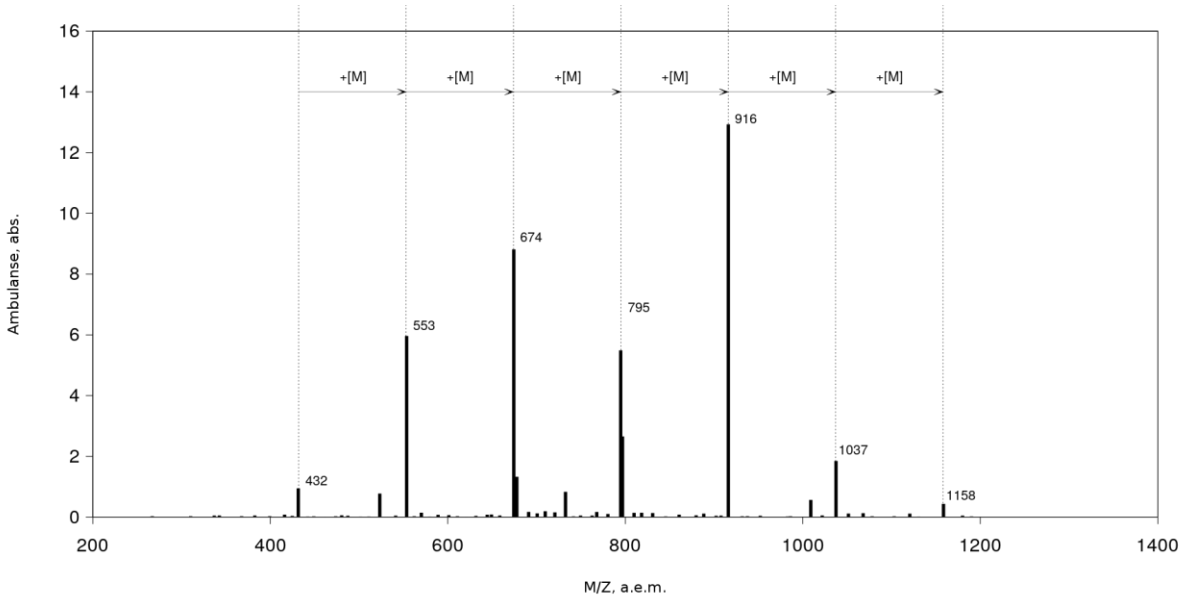

Figure S19. The chromatogram and the decomposition products of DS **1a** according to LC-MS data (ESI, Positive mode), M=$NO_2C_6H_3$.

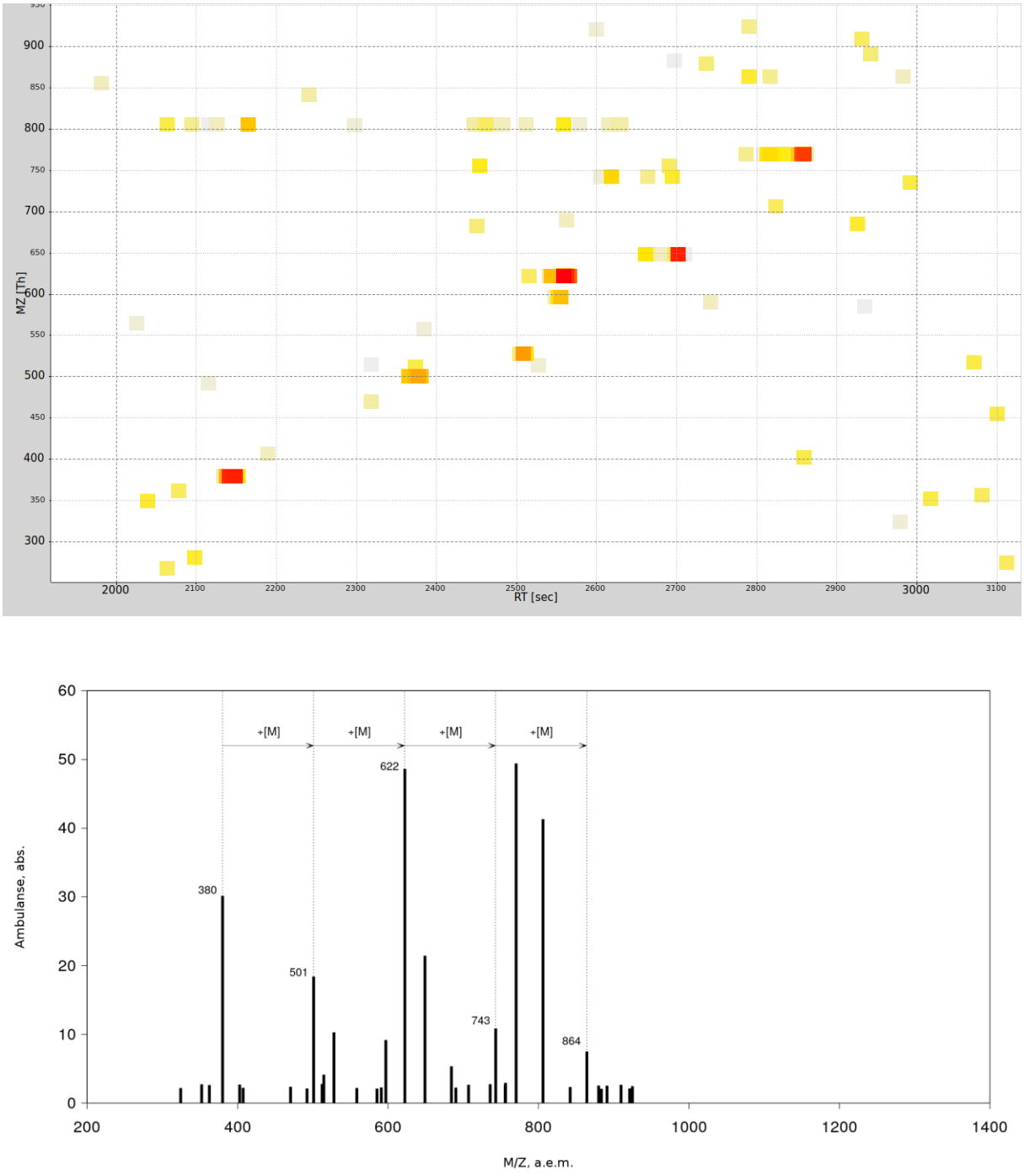

Figure S20. The chromatogram and the decomposition products of DS **1a** according to LC-MS data (ESI, Negative mode), M=$NO_2C_6H_3$.

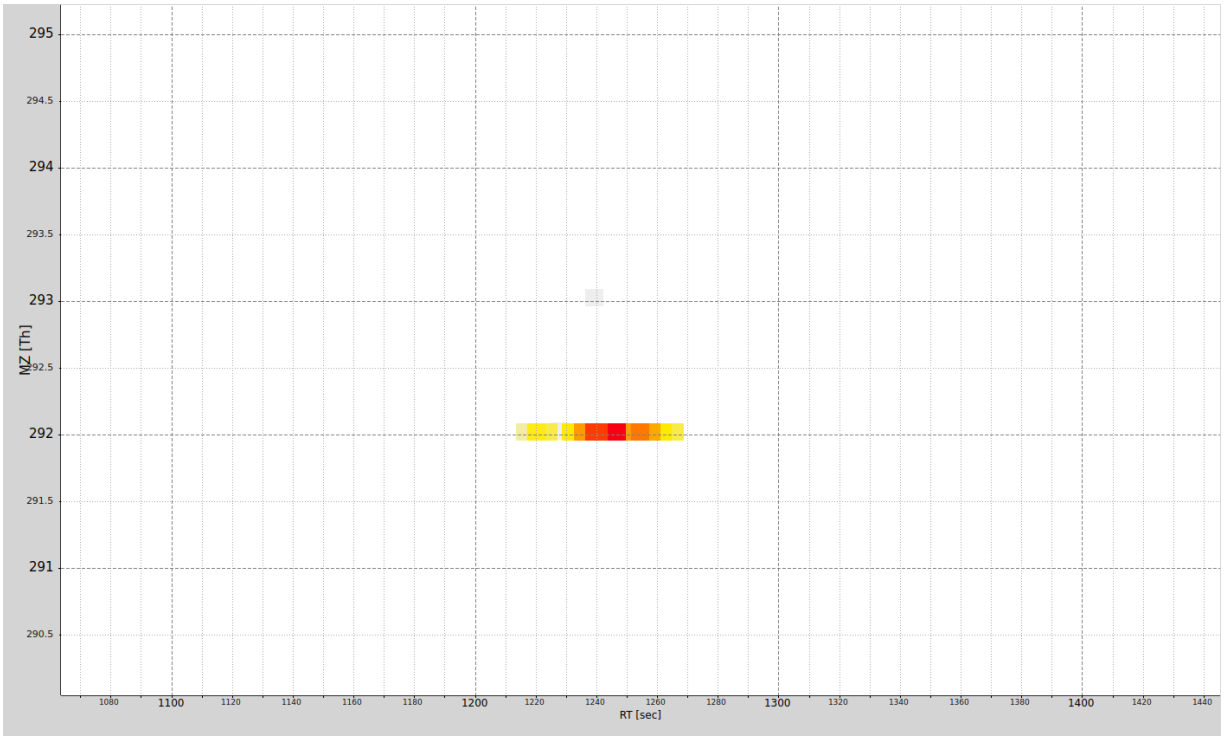

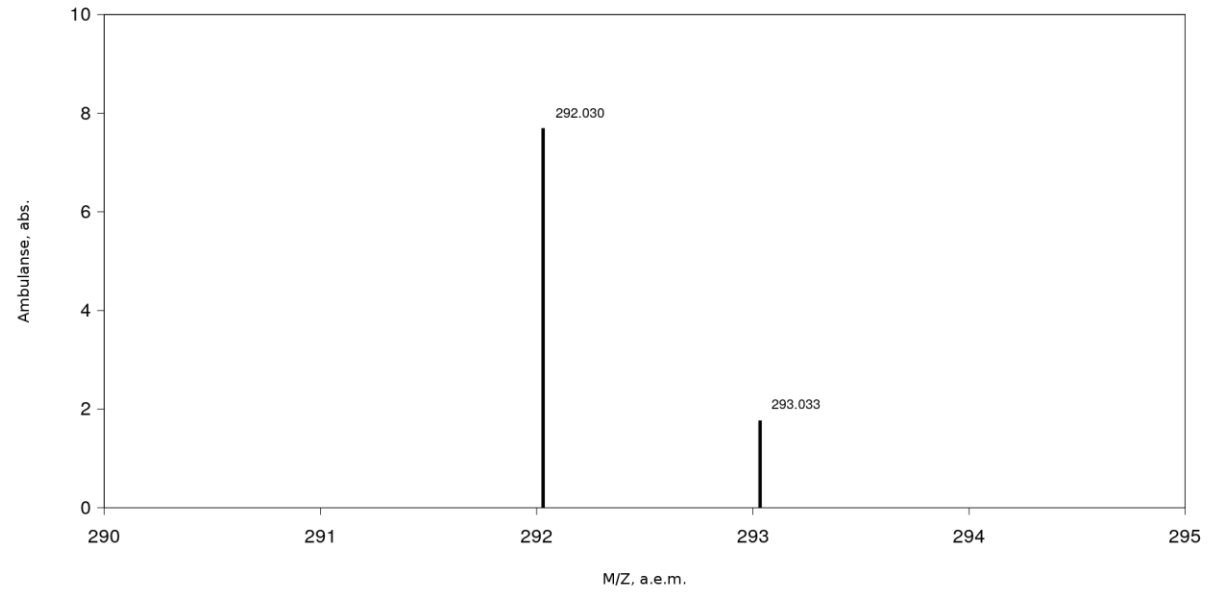

Figure S21. The chromatogram and the decomposition products of DS **2** according to LC-MS data (ESI, Negative mode).